WARSAW UNIVERSITY OF TECHNOLOGY Index 351733
FACULTY OF CIVIL ENGINEERING
COMMITTEE FOR CIVIL AND WATER ENGINEERING
POLISH ACADEMY OF SCIENCES ISSN 1230-2945

DOI: 10.24425/ace.2025.155102

ARCHIVES OF CIVIL ENGINEERING

Vol. LXXI ISSUE 3 2025

pp. 325–338

Research paper

Exploring the potential: auxetic metamaterials as core elements in buckling restrained braces

Hamza Basri[1], Abdelouahab Ras[2], Karim Hamdaoui[3], Piotr Wielgos[4]

Abstract: Buckling restrained braces (BRBs) are now widely used in different seismic zones as lateral resisting systems due to their quasi-symmetric and stable cyclic behavior. These systems are capable of dissipating the energy of severe lateral loads while protecting the integrity of other components of the structure. The material selection for these damper components as the inner core element requires high ductility, low strength increase, and high energy dissipation ability. Therefore, designing BRB steel cores using auxetic metamaterials has been recently investigated and suggested in the field of structure protection. The behavior of these metamaterials is characterized by a negative Poisson's ratio (NPR) and unique mechanical characteristics, including their shear resistance and high ability for energy absorption. In this paper, we seek to investigate the effect of auxetic behavior on the dissipative performance of BRB under cyclic loading. Two different types of BRB were numerically designed and modeled using the finite element program Abaqus. The numerical analysis results show stable hysteresis behavior in both specimens and good stress distribution along the inner auxetic core. In addition, a parametric study was conducted to further investigate the effect of the gap size between the auxetic core and the concrete encasement. The cyclic performance of a buckling restrained brace with an auxetic perforated core was assessed, and the outcomes of this numerical analysis provide a reasonable basis for applying an auxetic core in the field of structure protection.

Keywords: auxetic core, buckling restrained brace, cyclic test, energy absorption, hysteresis behavior

[1]MSc., Eng., EOLE, Department of Civil Engineering, University of Tlemcen, BP 230, Tlemcen, Algeria, e-mail: hamza.basri@univ-tlemcen.dz, ORCID: 0000-0001-8465-7015
[2]DSc., PhD., Eng., EOLE, Department of Civil Engineering, University of Tlemcen, BP 230, Tlemcen, Algeria, e-mail: ouhab_ras@yahoo.fr, ORCID: 0000-0002-9178-0764
[3]DSc., PhD., Eng., EOLE, Department of Civil Engineering, University of Tlemcen, BP 230, Tlemcen, Algeria, e-mail: karim@unipv.it, ORCID: 0000-0002-2263-3138
[4]DSc., PhD., Eng., Department of Structural Mechanics, Lublin University of Technology, Lublin, Poland, e-mail: p.wielgos@pollub.pl, ORCID: 0000-0003-3548-9945

1. Introduction

The field of materials science has unveiled a novel category of materials known as Auxetic Metamaterials, often referred to as 'auxetics' by Evens [1,2], due to their unique characteristics of negative Poisson's ratio (NPR). These materials exhibit a peculiar and counterintuitive property: when stretched, they expand laterally rather than contracting, making them unique among their conventional materials [3–5]. This inherent property endows Auxetic Metamaterials with extraordinary mechanical characteristics, rendering them highly promising for a multitude of applications, including structural engineering. Auxetic meta-structures have been reported to be generated by the NPR, with a variety of enhanced mechanical features in shear, indentation, crushing, fatigue, and energy absorption [6–10]. Therefore, there are many potential applications for auxetic meta-structures in a variety of domains, such as biomedicine [11], aerospace [12], textiles [13], military [14], as well as some tools needed in our daily life [15].

Recent advancements in auxetics metamaterials have led to a deeper understanding of their underlying principles and the development of novel structures and applications [16,17]. Researchers have been focusing on creating intricate designs, with a particular emphasis on re-entrant structures such as the re-entrant honeycomb, which have garnered significant attention due to their exceptional properties [18,19]. Numerous research papers have been made to develop and further investigate the re-entrant honeycomb and their applications in various fields. The possibility of auxetic metamaterials to absorb energy and protect structures from massive seismic events has been studied [20]. Xiao et al [21] created two different types of graded auxetic reentrant hexagonal honeycombs to examine the impact of the gradient distribution on the deformation mode. A modified re-entrant honeycomb auxetic structure is presented by Mustahsan et al [22], in order to improve the structure's overall regulation, a third horizontal member is inserted between the vertical and re-entrant members of the semi-reentrant honeycomb type to increase the negative Poisson's ratio's (NPR) values. When subjected to static loads, these structures exhibit good auxetic behavior and load-carrying ability [23,24]. Considering their ability for absorbing energy and fracture resistance capacity, auxetic materials and structures have great potential to protect infrastructure from earthquake disasters [25]. However, very few studies have been reported to date on the use of these metamaterials on the field of seismic protection systems.

A perforated all-steel BRB with an auxetic core was first proposed for exploring the seismic behaviour of these modern meta-materials and their ability to dissipate energy [26]. A new design of all-steel BRB with a negative Poisson's ratio perforated core (NP-BRB) was proposed and experimentally studied. The results showed the advantages of using an auxetic perforated core instead of a solid steel core, including stable hysteresis performance and better energy dissipation. Numerical analysis shows that both out-of-plane and in-plane deformations can be enhanced due to the improved auxetic behaviour. Zhang et al [27] modeled and tested a novel buckling-induced planner isotropic auxetic meta-structure by arraying orthogonal tri-dumbbell holes into a sheet structure. The proposed model exhibits better aseismic performance with excellent auxeticity in relatively significant deformations. Zhu et al [28] develop new types of BRB using two forms of perforated auxetic structures, including ellipse and peanut-shaped

structures. Hamed et al [29], Wang et al [30] proposed novel steel plate shear wall SPWS with auxetic perforated core plates, The results improve and support the use of auxetic-shaped SPSWs as effective energy dissipation devices due to their good hysteretic behavior and light weights. More research is needed to fully understand the effects of auxetics on the cyclic behavior and the dissipative performance of various seismic devices. However, the available evidence suggests that auxetic metamaterials have the potential to revolutionize seismic protection systems.

Buckling Restrained Brace (BRB), a seismic retrofitting and structural engineering innovation, has emerged as a critical element in enhancing the resilience and safety of buildings and infrastructure subjected to earthquake forces [31,32]. Extensive study has been done on such systems to improve the BRB's aseismic performance due to its stable hysteretic performance [33–35]. Unlike conventional braces, which may experience local buckling and exhibit brittle behavior under extreme loading conditions, BRBs incorporate an ingenious restraint system that prevents premature buckling. A series of works have been conducted for further understanding of the BRBs mechanism at the component level including the steel core length variation [36], different core widths [37], buckling restrained mechanisms [38], unbounding material [39], stoppers [40], lateral thrust [41], discontinuous restraint [42]. Despite the fact that conventional BRBs have several benefits, their substantial weight makes transporting and installation difficult [43]. As a result, numerous studies on BRBs were done, and various materials and techniques were suggested for improving some of these concerns with the brace [44, 45].

The primary force-carrying component of BRBs is the core brace. Some studies attempt to introduce steel plates with perforated holes as BRB brace to enter the plastic state more rapidly and undergo rapid yielding to achieve increased energy dissipation capacity [46, 47]. A unique BRB with NPR perforated core was designed by Zhang et al. [26] using a bulking-induced auxetic meta-structure, which is proven to have stable hysteretic curves and a small compression strength adjustment factor. Piedrafita et al [48] tested a new perforated core BRB with stable hysteretic properties, high ductility, and increased energy dissipation capacity. Furthermore, by incorporating innovative materials such as shape memory alloy into BRBs to enhance the energy dissipation and centering capabilities [49, 50]. Fiber-reinforced polymers (FRPs) are also used into BRBs due to their ability to increase the ductility, and load-bearing capacity, and enhance the seismic behavior of members [51, 52]. Fang et al. [53] analyze the seismic performance of various BRBs with different cross-section types and different gaps using quasi-static tests. The study reveals that all BRB types demonstrate good hysteretic performance, with cross-type configurations showing higher load-bearing capacity and energy consumption. Carbon fiber specimens exhibited breakage under lateral thrust, indicating the need for additional restraints like steel hoops or stirrups for better performance. The aforementioned findings demonstrate that high-performance BRBs have been extensively researched for their seismic resistance, although the auxetic structure and traditional BRBs are still in the early stages of experiments. Inspired by the recent research, in this paper, we aim to investigate the dissipative behavior of two types of BRB with a re-entrant auxetic core. A numerical analysis was conducted using a finite element program, both BRB types are equipped with the same auxetic characteristics, and test results were compared and discussed.

2. FEM modeling

Two numerical models of Buckling Restrained Brace with auxetic steel core were modeled and analyzed using the finite element method. The perforated steel core with re-entrant honeycomb unit cells was controlled by regarding three geometrical parameters, hole ratio, length and the corner angle of the unit cells. As shown in Fig. 1, two different concepts were presented and will be used for a numerical investigation of energy dissipation capacity and hysteresis behavior. Each BRB featuring an identical steel inner core but differing in their encasing systems. One BRB utilizes an entirely steel encasing, providing a more compact and potentially lighter solution. In contrast, the other BRB employs a concrete encasing, adding mass and stiffness to enhance energy dissipation.to compare the impact of casing system on the hysteresis behavior of the inner auxetic core.

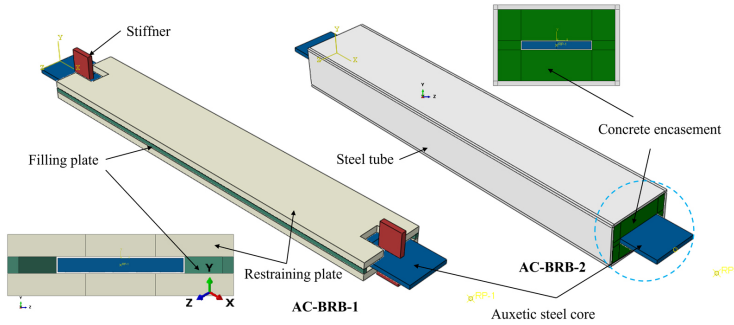

Fig. 1. Members and Assembly of AC-BRB-1 and AC-BRB-2

The auxetic core characteristics were kept the same for the two models, including the same steel core thickness of 10 mm, the same length of perforated area of 540 mm. The two models have the same cross section value of 320 mm², and the re-entrant honeycomb were set perpendicularly to the cyclic loading direction. The geometrical dimensions of the re-entrant honeycomb cells are shown in Fig. 2, along with the detailed dimensions of all buckling restrained brace components in Fig. 3.

The assembly of the auxetic core-buckling restrained braces AC-BRB was designed with the consideration of the overall buckling prevention design condition using the safety factor ν_F which is given by the following equation [54]:

$$\nu_F = \frac{1}{\dfrac{P_y}{P_E^R} + \left(\dfrac{P_y L}{M_y^R} \cdot \dfrac{a+d+e}{L}\right)} \geq 3.0 \tag{2.1}$$

$$P_y = F_y \cdot A_s \tag{2.2}$$

$$P_E^R = \frac{\pi^2 E^R I^R}{L^2} \tag{2.3}$$

where, P_y is the yield load of the inner core and P_E^R is the Euler buckling load of the restraining members which could be calculated by Eq. (2.2), and Eq. (2.3), respectively, L is the length of

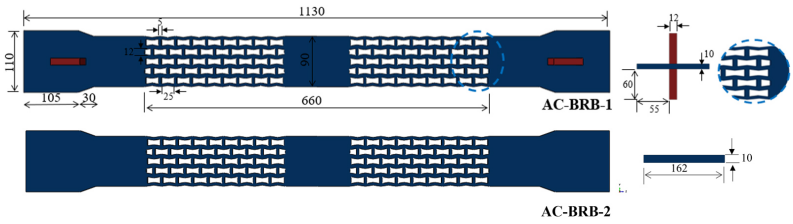

(a)

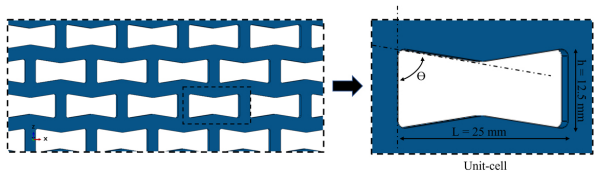

(b)

Fig. 2. Details of AC-BRB auxetic core: (a) Auxetic perforated cores, (b) Geometric details of the re-entrant honeycomb structure

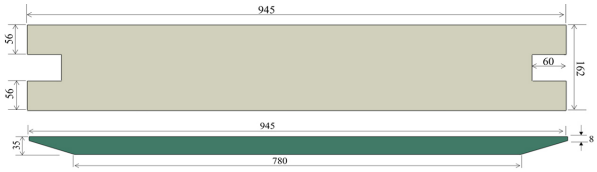

(a)

(b)

Fig. 3. Details of AC-BRBs restraining components: (a) AC-BRB-1, (b) AC-BRB-2

the yielding segment of the steel core, M_y^R is the yield moment of the restraining plates, d represents the gap between the steel core and the restraining plates, a is the initial imperfection at mid-length of the BRB; and e is the eccentricity of axial load, a and e are considered as $L/1000$ in this study. F_y is the yield stress of the core material and A_s is the area of cross section, $E^R$and $I^R$are young's modulus and the inertial moment, respectively.

The two steel components material was utilized for the numerical analysis, with both the steel core and steel tube fabricated from the same steel grade, Q235b. The mass density, elastic properties, and plastic characteristics of this material is detailed in Table 1. The Chaboche

model, which accounts for the Bauschinger effect, describes the material behavior under cyclic loading, with necessary factors such as γ and C provided in Table 2. Unlike the steel core material, the steel tube material is not expected to exhibit plasticity.

Table 1. Mechanical Properties of Q235b

Material	**Young modulus (GPa)**	**Yield stress (MPa)**	**Yield strain (MPa)**	**Ultimate stress (MPa)**	**Ultimate strain (MPa)**
Q235b	208.4	284	0.0013	416	0.39

Table 2. The Chaboche model properties of Q235b

Material	σ_y	Q_∞	b	C_1	γ_1	C_2	γ_2	C_3	γ_3
Q235b	284	10	1.2	100000	2500	7500	100	500	0

The contact between the auxetic core and the concrete encasement was assumed to have high stiffness in the transvers direction and tangential coulomb frictional behaviour with a friction coefficient of 0.3. The contact model allowed the auxetic core to move freely during the loading and unloading, which enabled higher buckling modes. Moreover, tie constraints were added between the concrete and the steel tube to ensure that they behave as unique part during the loading process.

All the model components are made using 3D solid elements. Eight-node elements with reduced integration (C3D8R) was selected regarding that this element type improves its analysis precision and computational efficiency at highly nonlinear demand. To achieve more accurate structural discretization, the partitions tool was used. The model's components were meshed using 10 mm mesh. To capture the significant deformation predicted along the steel core, three elements were applied in the thickness direction. In term of the boundary conditions applied, the brace was fixed at the left end, and then loaded at the right end using a coupling reference point. The loading procedure in this case is considered as nonlinear static general applied to the right end of the brace as cyclic loading. Fig. 4, shows the loading protocol consists of 4 different amplitudes, each amplitude was repeated 3times which are L/300, L/200, L/150, and L/100, respectively.

3. FEM results

Figure 5 depicts the axial force-displacement curve of the both models AC-BRB-1 and AC-BRB-2. Both models exhibit stable, symmetrical and smooth hysteresis loops during the four amplitudes cycles loading, except for the last loading cycles, when the auxetic core shows a rippling under compression loads, leading to a sharp degradation in stiffness especially for the specimen AC-BRB-2. The stiffness degradation in the last cycles resulted from a large friction force that develops at the gap zone between the auxetic core and its surrounded restraining elements. The skeleton curve of both models is also illustrated, which is obtained by collecting

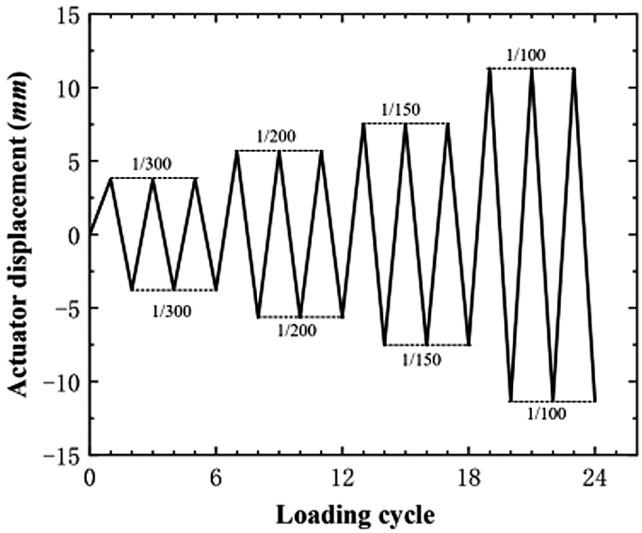

Fig. 4. Loading Protocol

the maximum force and displacement values in every loading cycle. Based on the results, the maximum force of AC-BRB-1 and AC-BRB-2 were 145.06 kN and 138.353 kN in tension, and 154.54 kN and 140.204 kN in compression, respectively (Fig. 5).

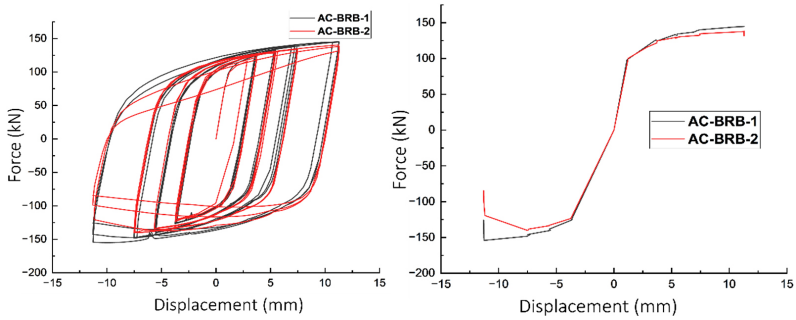

Fig. 5. Hysteresis curve and skeleton curve of AC-BRB models

Through the analysis of the hysteresis behavior of AC-BRB specimens, different performance indices can be obtained such as the equivalent viscous damping factor ξ_{eq}, the compression strength adjustment factor β, and the stiffness degradation K_i. An equivalent viscous damping ratio ξ_{eq} is used to evaluate the ability of the two specimens to dissipate energy, calculated based on Fig. 6c, and Eq. (3.1):

$$\xi_{\text{eq}} = \frac{1}{2\pi} \frac{S_{\text{AFDEA}}}{S_{\Delta\text{OAB}} + S_{\Delta\text{OCD}}} \tag{3.1}$$

where, S_{FDEA} is the area enclosed per hysteresis loop representing the entire dissipated energy, and $S_{\Delta\text{OAB}}$ $S_{\Delta\text{OCD}}$ represent the area of elastic strain energy.

The variation in the equivalent viscous damping ratio ξ_{eq} is shown in Fig. 6a, the values of ξ_{eq} for AC-BRB-1 and AC-BRB-2 increase with the increase of deformation. The ξ_{eq} values decrease greatly during the last two cycles to 0.32 and 0.30 for AC-BRB-1 and AC-BRB-2 respectively. The reason is that the auxetic core exhibits local buckling due to a large friction force at the contact zone for the two specimens under the last amplitude corresponds to the pinching effect in the hysteresis curves in Fig. 5. The values of secant stiffness $K_i$of both models are also extracted from the hysteresis curves using the Eq. (3.2):

$$K_i = \frac{|Fi^+| + |Fi^-|}{|\Delta i^+| + |\Delta i^-|} \tag{3.2}$$

where, Fi and Δi are the maximum load and deformation in each $i-$th loop cycle. A_s illustrated in Fig. 6b, there is a slight difference in the secant stiffness of the AC-BRB-1 and AC-BRB-2, and the stiffness values of the two specimens are degrading up to 12.4 and 11.27 for AC-BRB-1 and AC-BRB-2 respectively.

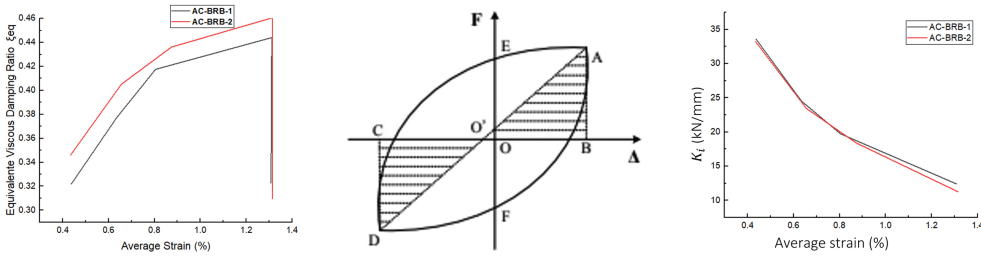

(a) (b) (c)

Fig. 6. Energy dissipation capacity of AC-BRB models: (a) Equivalent viscous damping ratio ξ_{eq}, (b) Secant stiffness K_i, (c) Calculation of the dissipated energy

Table 3 summarized the main computational numerical results of the two tested AC-BRB specimens. These mechanical properties including maximum values of tension and compression, the compression strength adjustment factor β, the strain hardening adjustment factor ω, the maximum displacement ductility μ, and Cumulative plastic deformation factor (CPD).

AC-BRB-1 shows the maximum value of the displacement ductility μ of 9.94, whilst the value of μ for AC-BRB-2 is slightly less but still exceeds the value of 9. For the *CPD* values, both specimens exceed the required cumulative ductility value of 200, which conforms to the code design specification [55]. Thus, all the tested specimens indicating favourable ductility and good energy dissipation performance.

Figure 7 represent the von mises stresses of the AC-BRB components. The failure process of AC-BRB-1 and AC-BRB-2 occurred in the right side of the perforated segment under the last compression half cycle. The high frictional forces, generated at the zone auxetic core-restraints, could cause this phenomenon. This might explain the sudden decrease in the force-displacement values of the two specimens, AC-BRB-1 and AC-BRB-2, in the hysteresis

Table 3. Numerical results of the tested AC-BRB models

Specimens	C_{max}	T_{max}	B(C_{max}/ T_{max})	Δ_{max}	P_y	Δy	$\omega(T_{max}/P_y)$	$\mu(\Delta_{max}/\Delta y)$	***CPD***
AC-BRB-1	-154.45	144.67	1.06	11.24	98.15	1.13	1.47	9.94	245.66
AC-BRB-2	-140.20	138.35	1.01	11.29	100.25	1.24	1.38	9.11	221.67

curves shown in the Figure 5. The numerical results of AC-BRB-1 and AC-BRB-2 show that the stress concentration located at the horizontal perforated segments of the re-entrant honeycomb unit cells. This is most pronounced at the necking regions between the re-entrant honeycomb unit edges and the edge end of the auxetic core, due to the smallest cross-section in this region. The deformation of the restraining elements was also captured. As the loading continuous on the last cycles, the Von-Mises stress values for both BRB restraining mechanisms and the brace ends are significantly lower than the steel core's yielding strength, except for regions that exhibit sharp friction with the auxetic core, more clearly for the AC-BRB-2. This means that the connection zones and most regions of the restraining parts are in an elastic state and possess sufficient margin to prevent the local buckling.

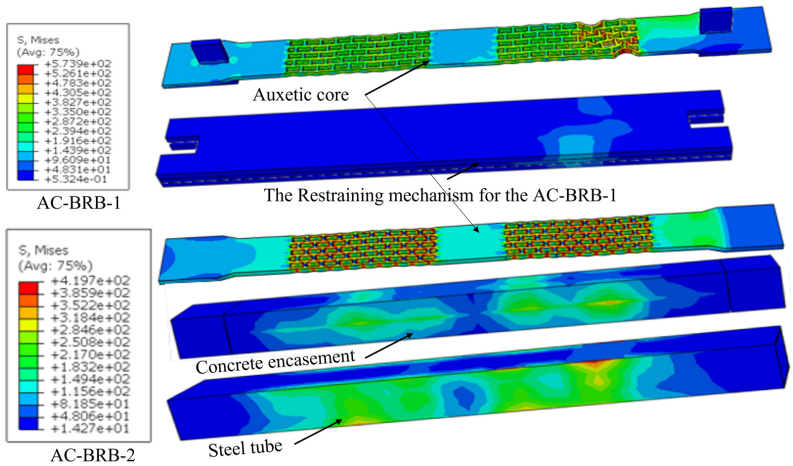

Fig. 7. The von Mises stress distribution of AC-BRB components (auxetic core and restraining parts)

In a parametric study, the gap size between the auxetic core and the concrete encasement was investigated. Three specimens with 1mm, 2 mm, and, 2.5 mm were modeled and analyzed. The hysteresis curves are given in Fig. 8, it is observed from the hysteresis loops that the pinching effect increases as the gap size increases particularly for the compression regions. It should be mentioned that when the gap size is 3mm or more, the model calculation fails to achieve convergence. The phenomenon is caused by the fact that when the gap increases, this would result in more visible local buckling of the inner core, hence, a stiffness degradation of the core is developed. On the other, an excessively reduced gap would result in the Poisson effect, meaning the lateral deformation of the core unit as a direct result of its vertical displacement.

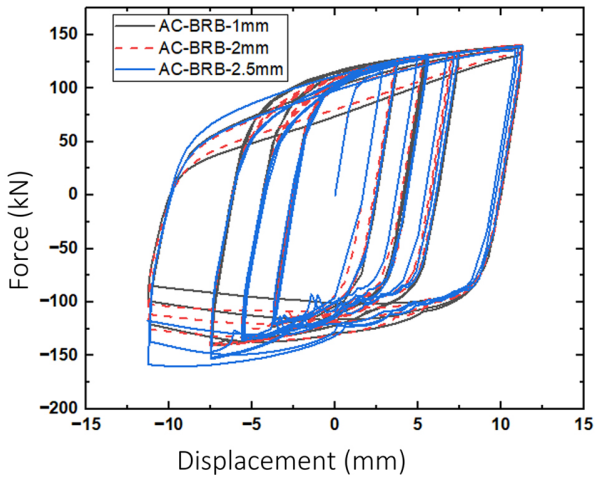

Fig. 8. The hysteresis curve comparison of AC-BRB with different gap size

4. Conclusions

In the present study, two different specimens of buckling restrained braces with an auxetic core (AC-BRB) were modeled and investigated. The re-entrant honeycomb configuration was modeled and analyzed based on the finite element method to investigate the hysteresis behavior and explore the performance dissipative of the auxetic core under cyclic loading. The study results could be summed up as follows:

- Based on the numerical test results, both specimens exhibit stable, symmetrical, and smooth hysteresis behavior during the first three amplitudes without overall buckling, which was observed at the second half of the last amplitude cycle for the AC-BRB-2;
- All the specimens show excellent and stable performance in terms of the strength, ductility and energy dissipation ability;
- The respective CPD values of AC-BRB1, AC-BRB2 are 245, 221. Both meet the AISC341-10 requirement;
- The failure modes of AC-BRB are caused by local buckling located in the perforated segment at the second half of the last cyclic loading, resulting from stress concentration around the re-entrant honeycomb unit cells;
- According to the parametric study for the gap size, it was found that a gap size of 2.5 mm had the highest effect on the hysteresis behavior of the BRB system. However, Increasing the gap between auxetic core and restraining parts would make the pinch and fluctuation of hysteretic curves more obvious, especially for the compression parts of the curves.

References

[1] K.E. Evans, “Auxetic polymers: a new range of materials”, *Endeavour*, vol. 15, no. 4, pp. 170–174, 1991, doi: 10.1016/0160-9327(91)90123-S.

[2] K.E. Evans, M.A. Nkansah, I.J. Hutchinson, and S.C. Rogers, "Molecular network design", *Nature*, vol. 353, art. no. 124, 1991, doi: 10.1038/353124a0.

[3] X. Ren, R. Das, P. Tran, T.D. Ngo, and Y.M. Xie, "Auxetic metamaterials and structures: A review", *Smart Materials and Structures*, vol. 27, no. 2, 2018, doi: 10.1088/1361-665X/aaa61c.

[4] W. Wu, P. Liu, and Z. Kang, "A novel mechanical metamaterial with simultaneous stretching- and compression-expanding property", *Materials and Designe*, vol. 208, art. no. 109930, 2021, doi: 10.1016/j.matdes.2021.109930.

[5] N.K. Choudhry, B. Panda, and S. Kumar, "In-plane energy absorption characteristics of a modified re-entrant auxetic structure fabricated via 3D printing", *Composites Part B: Engineering*, vol. 228, art. no. 109437, 2022, doi: 10.1016/j.compositesb.2021.109437.

[6] X.Y. Zhang, X. Ren, X.Y. Wang, Y. Zhang, and Y.M. Xie, "A novel combined auxetic tubular structure with enhanced tunable stiffness", *Composites Part B: Engineering*, vol. 226, 2021, doi: 10.1016/j.compositesb.2021.109303.

[7] R. Critchley, I. Corni, J.A. Wharton, F.C. Walsh, R.J.K. Wood, and K.R.nStokes, "A review of the manufacture, mechanical properties and potential applications of auxetic foams", *Physica Status Solidi B*, vol. 250, no. 10, pp. 1963–1982, 2013, doi: 10.1002/pssb.201248550.

[8] G. Imbalzano, S. Linforth, T.D. Ngo, P.V.S. Lee, and P. Tran, "Blast resistance of auxetic and honeycomb sandwich panels: Comparisons and parametric designs", *Composite Structures*, vol. 183, no. 1, pp. 242–261, 2018, doi: 10.1016/j.compstruct.2017.03.018.

[9] F. Scarpa, J.A. Giacomin, A. Bezazi, and W.A. Bullough, "Dynamic behavior and damping capacity of auxetic foam pads", *Smart Structures and Materials 2006: Damping and Isolation. Proceedings SPIE,* vol. 6169, art. no. 61690T, 2006, doi: 10.1117/12.658453.

[10] Y. Zhang, et al., "Static and dynamic properties of a perforated metallic auxetic metamaterial with tunable stiffness and energy absorption", *International Journal of Impact Engineering*, vol. 164, 2022, doi: 10.1016/j.ijimpeng.2022.104193.

[11] J. Li, Z.Y. Zhang, H.T. Liu, and Y.B. Wang, "Design and characterization of novel bi-directional auxetic cubic and cylindrical metamaterials", *Composite Structures*, vol. 299, art. no. 116015, 2022, doi: 10.1016/j.compstruct.2022.116015.

[12] C. Lira, F. Scarpa, and R. Rajasekaran, "A gradient cellular core for aeroengine fan blades based on auxetic configurations", *Journal of Intelligent Material Systems and Structures*, vol. 22, no. 9, pp. 907–917, 2011, doi: 10.1177/1045389X11414226.

[13] Z. Wang and H. Hu, "Auxetic materials and their potential applications in textiles", *Textile Research Journal*, vol. 84, no. 15, pp. 1600–1611, 2014, doi: 10.1177/0040517512449051.

[14] R.P. Bohara, S. Linforth, T. Nguyen, A. Ghazlan, and T. Ngo, "Dual-mechanism auxetic-core protective sandwich structure under blast loading", *Composite Structures*, vol. 299, 2022, doi: 10.1016/j.compstruct.2022.116088.

[15] J. Smardzewski, D. Jasińska, and M. Janus-Michalska, "Structure and properties of composite seat with auxetic springs", *Composite Structures*, vol. 113, no. 1, pp. 354–361, 2014, doi: 10.1016/j.compstruct.2014.03.041.

[16] R. Galea, P.S. Farrugia, K.K. Dudek, D. Attard, J.N. Grima, and R. Gatt, "A novel design method to produce 3D auxetic metamaterials with continuous pores exemplified through 3D rotating auxetic systems", *Materials and Design*, vol. 226, art. no. 111596, 2023, doi: 10.1016/j.matdes.2023.111596.

[17] D. Han, et al., "Lightweight auxetic metamaterials: Design and characteristic study", *Composite Structures*, vol. 293, 2022, doi: 10.1016/j.compstruct.2022.115706.

[18] S.Z. Khan, S.H. Masood, and R. Cottam, "Mechanical properties in tensile loading of H13 re-entrant honeycomb auxetic structure manufactured by direct metal deposition", *MATEC Web of Conferences*, vol. 34, pp. 1–4, 2015, doi: 10.1051/matecconf/20153401004.

[19] A. Alomarah, J. Zhang, D. Ruan, S. Masood, and G. Lu, "Mechanical Properties of the 2D Re-entrant Honeycomb Made via Direct Metal Printing", *IOP Conference Series: Materials Science and Engineering*, vol. 229, 2017, doi: 10.1088/1757-899X/229/1/012038.

[20] S. Brűlé, S. Enoch, and S. Guenneau, "Emergence of seismic metamaterials: Current state and future perspectives", *Physics Letters A,* vol. 384, no. 1, art. no. 126034, 2020, doi: 10.1016/j.physleta.2019.126034.

[21] D. Xiao, Z. Dong, Y. Li, W. Wu, and D. Fang, "Compression behavior of the graded metallic auxetic reentrant honeycomb: Experiment and finite element analysis", *Materials Science and Engineering: A,* vol. 758, pp. 163–171, 2019, doi: 10.1016/j.msea.2019.04.116.

[22] F. Mustahsan, S.Z. Khan, A.A. Zaidi, Y.H. Alahmadi, E.R.I. Mahmoud, and H. Almohamadi, "Re-Entrant Honeycomb Auxetic Structure with Enhanced Directional Properties", *Materials (Basel)*, vol. 15, no. 22, 2022, doi: 10.3390/ma15228022.

[23] C. Qi, et al., "Quasi-static crushing behavior of novel re-entrantmcircular auxetic honeycombs", *Composites Part B: Engineering*, vol. 197, art. no. 108117, 2020, doi: 10.1016/j.compositesb.2020.108117.

[24] Y. Zhou, Y. Li, D. Jiang, Y. Chen, Y. Min Xie, and L. J. Jia, "In-plane impact behavior of 3D-printed auxetic stainless honeycombs", *Engineering Structures*, vol. 266, art. no. 114656, 2022, doi: 10.1016/j.engstruct.2022.114656.

[25] B. Ungureanu, Y. Achaoui, S. Enoch, S. Brűlé, and S. Guenneau, "Auxetic-like metamaterials as novel earthquake protections", *EPJ Applied Metamaterials*, vol. 2, 2015, doi: 10.1051/epjam/2016001.

[26] Y. Zhang, X. Ren, X.Y. Zhang, T.T. Huang, L. Sun, and Y.M. Xie, "A novel buckling-restrained brace with auxetic perforated core: Experimental and numerical studies", *Engineering Structures*, vol. 249, 2021, doi: 10.1016/j.engstruct.2021.113223.

[27] Q. Zhang, Y. Zhu, F. Lu, C. Yu, X. Ren, and Y. Shao, "A novel buckling-induced planner isotropic auxetic meta-structure and its application in BRB: A numerical study", *Mechanics of Advanced Materials and Structures*, vol. 31, no. 24, pp. 1–14, 2024, doi: 10.1080/15376494.2023.2224810.

[28] Y. Zhu, J. Wang, X. Cai, Z. Xu, and Y. Wen, "Cyclic behavior of ellipse and peanut-shaped perforated buckling-restrained braces", *Engineering Structures*, vol. 291, art. no. 116432, 2023, doi: 10.1016/j.engstruct.2023.116432.

[29] A.A. Hamed, R.B. Asl, and H. Rahimzadeh, "Experimental and numerical study on the structural performance of auxetic-shaped, ring-shaped and unstiffened steel plate shear walls", *Journal of Building Engineering*, vol. 34, art. no. 101939, 2021, doi: 10.1016/j.jobe.2020.101939.

[30] J. Wang, Y. Zhu, and X. Cai, "Numerical modeling of seismic behavior of ellipse and peanut-shaped auxetic steel plate shear walls", *Low-carbon Materials and Green Construction*, vol. 1, art. no. 10, 2023, doi: 10.1007/s44242-023-00011-9.

[31] J. Kim and H. Choi, "Behavior and design of structures with buckling-restrained braces", *Engineering Structures*, vol. 26, no. 6, pp. 693–706, 2004, doi: 10.1016/j.engstruct.2003.09.010.

[32] L.A. Fahnestock, R. Sause, J.M. Ricles, and L.W. Lu, "Ductility demands on buckling-restrained braced frames under earthquake loading", *Earthquake Engineering and Engineering Vibration*, vol. 2, no. 2, pp. 255–268, 2003, doi: 10.1007/s11803-003-0009-5.

[33] P. Saingam, et al., "Composite behavior in RC buildings retrofitted using buckling-restrained braces with elastic steel frames", *Engineering Structures*, vol. 219, art. no. 110896, 2020, doi: 10.1016/j.engstruct.2020.110896.

[34] C. Avci-Karatas, O.C. Celik, and C. Yalcin, "Experimental Investigation of Aluminum Alloy and Steel Core Buckling Restrained Braces (BRBs)", *International Journal of Steel Structures*, vol. 18, no. 2, pp. 650–673, 2018, doi: 10.1007/s13296-018-0025-y.

[35] C. Avci-Karatas, O.C. Celik, and S. Ozmen Eruslu, "Modeling of Buckling Restrained Braces (BRBs) using Full-Scale Experimental Data", *KSCE Journal of Civil Engineering*, vol. 23, no. 10, pp. 4431–4444, 2019, doi: 10.1007/s12205-019-2430-y.

[36] M. Mirtaheri, A. Gheidi, A.P. Zandi, P. Alanjari, and H.R. Samani, "Experimental optimization studies on steel core lengths in buckling restrained braces", *Journal of Constructional Steel Research*, vol. 67, no. 8, pp. 1244–1253, 2011, doi: 10.1016/j.jcsr.2011.03.004.

[37] F. Barbagallo, M. Bosco, E.M. Marino, and P.P. Rossi, "Achieving a more effective concentric braced frame by the double-stage yield BRB", *Engineering Structures,* vol. 186, pp. 484–497, 2019, doi: 10.1016/j.engstruct.2019.02.028.

[38] H.M. Yazdi, M. Mosalman, and A.M. Soltani, "Seismic Study of Buckling Restrained Brace System without Concrete Infill", *International Journal of Steel Structures*, vol. 18, no. 1, pp. 153–162, 2018, doi: 10.1007/s13296-018-0312-7.

[39] Q. Chen, C.L. Wang, S. Meng, and B. Zeng, "Effect of the unbonding materials on the mechanic behavior of all-steel buckling-restrained braces", *Engineering Structures*, vol. 111, pp. 478–493, 2016, doi: 10.1016/j.engstruct.2015.12.030.

[40] C.L. Wang, T. Usami, and J. Funayama, "Evaluating the influence of stoppers on the low-cycle fatigue properties of high-performance buckling-restrained braces", *Engineering Structures*, vol. 41, pp. 167–176, 2012, doi: 10.1016/j.engstruct.2012.03.040.

[41] F. Genna, "Lateral thrust in all-steel buckling-restrained braces: Experimental and FEM results", *Engineering Structures*, vol. 213, art. no. 110512, 2020, doi: 10.1016/j.engstruct.2020.110512.

[42] M.H. Mortezagholi and S.M. Zahrai, "Analytical and numerical studies on reducing lateral restraints in conventional & all steel Buckling Restrained Braces", *Journal of Building Engineering*, vol. 32, 2020, doi: 10.1016/j.jobe.2020.101513.

[43] ' K. Deng, P. Pan, X. Nie, X. Xu, P. Feng, and L. Ye, "Study of GFRP Steel Buckling Restraint Braces", *Journal of Composites for Construction*, vol. 19, no. 6, pp. 1–8, 2015, doi: 10.1061/(asce)cc.1943-5614.0000567.

[44] P. Dusicka and J. Tinker, "Global Restraint in Ultra-Lightweight Buckling-Restrained Braces", *Journal of Composites for Construction*, vol. 17, no. 1, pp. 139–150, 2013, doi: 10.1061/(asce)cc.1943-5614.0000320.

[45] J. Zhao, B. Wu, and J. Ou, "A novel type of angle steel buckling-restrained brace: cyclic behavior and failure mechanism", *Earthquake Engineering and Structural Dynamics*, vol. 40, no. 10, pp. 1083–1102, doi: 10.1002/eqe.1071.

[46] X. Cahís, E. Simon, D. Piedrafita, and A. Catalan, "Core behavior and low-cycle fatigue estimation of the Perforated Core Buckling-Restrained Brace", *Engineering Structures,* vol. 174, pp. 126–138, 2018, doi: 10.1016/j.engstruct.2018.07.044.

[47] Z. Yun, Y. Cao, J. Takagi, G. Zhong, and Z. He, "Experimental and numerical investigation of a novel all-steel assembled core perforated buckling-restrained brace", *Journal of Constructional Steel Research,* vol. 193, art. no. 107288, 2022, doi: 10.1016/j.jcsr.2022.107288.

[48] D. Piedrafita, X. Cahis, E. Simon, and J. Comas, "A new perforated core buckling restrained brace", *Engineering Structures*, vol. 85, pp. 118–126, 2015, doi: 10.1016/j.engstruct.2014.12.020.

[49] B. Asgarian and S. Moradi, "Seismic response of steel braced frames with shape memory alloy braces", *Journal of Constructional Steel Research*, vol. 67, no. 1, pp. 65–74, 2011, doi: 10.1016/j.jcsr.2010.06.006.

[50] A.F. Ghowsi, D.R. Sahoo, and P.C.A. Kumar, "Cyclic tests on hybrid buckling-restrained braces with Fe-based SMA core elements", *Journal of Constructional Steel Research*, vol. 175, art. no. 106323, 2020, doi: 10.1016/j.jcsr.2020.106323.

[51] M. Bashiri and V. Toufigh, "Numerical and experimental investigation on a BRB confined with partially carbon fiber reinforced polymer (CFRP)", *Engineering Structures*, vol. 223, 2020, doi: 10.1016/j.engstruct.2020.111150.

[52] M. Jia, X. Yu, D. Lu, and B. Lu, "Experimental research of assembled buckling-restrained braces wrapped with carbon or basalt fiber", *Journal of Constructional Steel Research*, vol. 131, pp. 144–161, 2017, doi: 10.1016/j.jcsr.2017.01.004.

[53] Y. Fang, L. Lv, Y. Gao, and Z. Fu, "Experimental of buckling restrained brace hysteretic performance with carbon fiber wrapped in concrete", *Archives of Civil Engineering*, vol. 70, no. 1, pp. 527–541, 2024, doi: 10.24425/ace.2024.148926

[54] T. Usami, H. Ge, and A. Kasai, "Overall buckling prevention condition of buckling-restrained braces as a structural control damper", in *14th World Conference on Earthquake Engineering, 12-17 Oct. 2008 Beijing, China*. [Online]. Available: http://www.iitk.ac.in/nicee/wcee/article/14_05-05-0128.PDF.

[55] AISC 341-10 Seismic Provisions for Structural Steel Buildings. American Institute of Steel Construction, 2010.

Odkrywanie potencjału: metamateriały auksetyczne jako elementy rdzenia w stężeniach z ograniczonym wyboczeniem

Słowa kluczowe: rdzeń auksetyczny, stężenia, próba cykliczna, absorpcja energii, pętla histerezy

Streszczenie:

Stężenia z ograniczonym wyboczeniem (Buckling Restrained Braces BRB) są obecnie szeroko stosowane w różnych strefach sejsmicznych jako boczne systemy nośne ze względu na ich quasi-symetryczne i stabilne zachowanie cykliczne. Systemy te są w stanie rozproszyć energię dużych obciążeń poprzecznych, chroniąc jednocześnie integralność innych elementów konstrukcji. Wybór materiału

na te elementy tłumika jako element rdzenia wewnętrznego wymaga wysokiej ciągliwości, niskiego wzrostu wytrzymałości i dużej zdolności rozpraszania energii. Dlatego też w ostatnim czasie badano i sugerowano projektowanie rdzeni stalowych BRB z wykorzystaniem metamateriałów auksetycznych w dziedzinie ochrony konstrukcji. Zachowanie tych metamateriałów charakteryzuje się ujemnym współczynnikiem Poissona (negative Poisson's ratio NPR) i unikalnymi właściwościami mechanicznymi, w tym odpornością na ścinanie i dużą zdolnością do pochłaniania energii. W tym artykule staramy się zbadać wpływ zachowania rdzenia auksetycznego na wydajność rozpraszającą BRB pod obciążeniem cyklicznym. Zaprojektowano numerycznie i zamodelowano dwa różne typy BRB przy użyciu programu elementów skończonych Abaqus. Wyniki analizy numerycznej wskazują na stabilne zachowanie histerezy w obu próbkach i dobry rozkład naprężeń wzdłuż wewnętrznego rdzenia auksetycznego. Ponadto przeprowadzono badanie parametryczne w celu dalszego zbadania wpływu rozmiaru szczeliny pomiędzy rdzeniem auksetycznym a obudową betonową. Oceniono cykliczną wydajność stężenia z ograniczonym wyboczeniem z auksetycznym perforowanym rdzeniem, a wyniki tej analizy numerycznej stanowią uzasadnioną podstawę do zastosowania rdzenia auksetycznego w dziedzinie ochrony konstrukcji.

Received: 2024-05-13, Revised: 2024-08-01